Early and Late M Intermediates in the Bacteriorhodopsin Photocycle: A Solid-State NMR Study†

Jingui G. Hu,‡,§ Boqin Q. Sun,‡,§ Marina Bizounok,‡ Mary E. Hatcher,‡,§ Jonathan C. Lansing,§ Jan Raap,|| Peter J. E. Verdegem,|| Johan Lugtenburg,|| Robert G. Griffin,§ and Judith Herzfeld*,‡,⊥

Department of Chemistry and Keck Institute for Cellular Visualization, Brandeis University, Waltham, Massachusetts 02254-9110, Department of Chemistry and Francis Bitter Magnet Laboratory, Massachusetts Institute of Technology, Cambridge, Massachusetts 02139, and Rijksuniversiteit te Leiden, 2300 RA Leiden, The Netherlands

Received December 29, 1997; Revised Manuscript Received March 19, 1998

ABSTRACT: To enforce vectorial proton transport in bacteriorhodopsin (bR), it is necessary that there be a change in molecular structure between deprotonation and reprotonation of the chromophore—i.e., there must be at least two different M intermediates in the functional photocycle. We present here the first detection of multiple M intermediates in native wild-type bacteriorhodopsin by solid-state NMR. Illumination of light-adapted [ζ-^{15}N-Lys]-bR at low temperatures shifts the ^{15}N signal of the retinal Schiff base (SB) downfield by about 150 ppm, indicating a deprotonated chromophore. In 0.3 M Gdn-HCl at pH 10.0, two different M states are obtained, depending on the temperature during illumination. The M state routinely prepared at the lower temperature, M_o, decays to the newly observed M state, M_n, and the N intermediate, as the temperature is increased. Both relax to bR_{568} at 0 °C. A unique reaction sequence is derived: $bR_{568}\rightarrow M_o\rightarrow(M_n+N)\rightarrow bR_{568}$. M_o and M_n have similar chemical shifts at [12-^{13}C]ret, [14-^{13}C]ret, and [ε-^{13}C]Lys216, indicating that M_n, like M_o, has a 13-cis and C=N anti chromophore. However, a small splitting in the [14-^{13}C]ret signal of M_o reveals that it has at least two substates. The 7 ppm greater shielding of the SB nitrogen in M_n compared to M_o suggests an increase in basicity and/or hydrogen bonding. Probing the peptide backbone of the protein, via [1-^{13}C]Val labeling, reveals a substantial structural change between M_o and M_n including the relaxation of perturbations at some sites and the development of new perturbations at other sites. The combination of the change in the protein structure and the increase in the pK_a of the SB suggests that the demonstrated $M_o\rightarrow M_n$ transition may function as the "reprotonation switch" required for vectorial proton transport.

Bacteriorhodopsin (bR)[1] is one of the retinal pigments found in the archae *Halobacterium salinarium*. The retinal is encapsulated by a bundle of seven transmembrane helices and forms a Schiff base (SB) with Lys216. Absorption of light by bR_{568} initiates a photocycle that includes a series of intermediates identified by time-resolved visible spectroscopy (see Figure 1). Some steps in the photocycle are irreversible, but equilibrium has been observed between K and L, L and M, M and N, and N and O (*1*−*9*). Coupled with the photocycle is proton transport from the cytoplasm to the extracellular solution. Vectorial proton movement is accomplished when the SB transfers its proton to Asp85, with access to the extracellular side through Glu204 (*10*−*13*), and recovers a proton from Asp96, with access to the cytoplasmic side (*14*, *15*). The key issues are the unidirectionality of

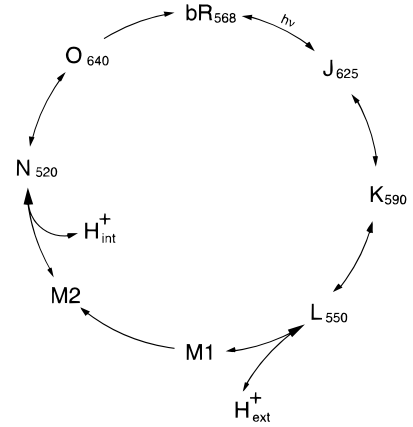

FIGURE 1: Photocycle of bR_{568}. The reversible reactions are represented by double-arrowed arcs and the unidirectional reactions by single-arrowed arcs. The irreversible transition from M1 to M2 is considered to be the "reprotonation switch" controlling proton pumping. To this end, it must change the connectivity of the SB from the extracellular side to the cytoplasmic side, while also increasing the pK_a of the SB.

† This research was supported by the National Institutes of Health (GM-36810 to J.H., GM-23289 and RR-00993 to R.G.G.).

* Corresponding author. Telephone: 781-736-2538. FAX: 781-736-2516. Email: herzfeld@brandeis.edu.

‡ Department of Chemistry, Brandeis University.

§ Massachusetts Institute of Technology.

|| Rijksuniversiteit te Leiden.

⊥ Keck Institute for Cellular Visualization, Brandeis University.

[1] Abbreviations: Asp, aspartic acid; bR, bacteriorhodopsin; bR_{568} or LA, the all-trans, 15-anti component of dark-adapted bR, the sole component of light-adapted bR, and the photon receptor for the proton motive photocycle; bR_{555}, the 13-cis, 15-syn component of dark-adapted bR; CP, cross-polarization; DA, dark-adapted bR, an ∼1:2 mixture of bR_{568} and bR_{555}; FTIR, Fourier transform infrared; Gdn-HCl, guanidine hydrochloride; Glu, glutamic acid; L, the intermediate preceding the M intermediates in the bR_{568} photocycle; M or M_x (x = 1, 2, o, n, etc.), intermediates in the bR_{568} photocycle with a deprotonated Schiff base; N, the intermediate following the M intermediates in the bR_{568} photocycle; Lys, lysine; MAS, magic angle spinning; NMR, nuclear magnetic resonance; Pro, proline; ret, retinal; SB, Schiff base; SSNMR, solid-state NMR; UV−Vis, ultraviolet−visible; Val, valine; WT, wild-type.

S0006-2960(97)03168-1 CCC: $15.00
Published on Web 05/08/1998

proton translocation, presumably controlled by an M1→M2 reaction, with associated structural changes in the chromophore and/or the protein (*16*−*18*).

Indirect experimental evidence for multiple M intermediates comes from detailed analysis of time-resolved visible spectra. Lanyi and co-workers have studied the kinetics of wild-type bR, mutants, and monomeric bR thoroughly and extensively (*6, 19*−*21*). From the simulation of kinetic data, they suggested a two-M model (*7, 8*), in which M_1 equilibrates with its precursor L, and M_2 equilibrates with its relaxation product N (*5*). The $M_1 \rightarrow M_2$ reaction is considered responsible for the change in the pK_a of the Schiff base, the transfer of the remaining free energy from the chromophore to the protein, the switch in access of the Schiff base to protons, and the unidirectionality of the photocycle (*18*). In monomeric bR, a slight difference is observed in the visible absorption of the two M's ($\lambda_{max} = 412$ nm for M_1 and $\lambda_{max} = 408$ nm for M_2) (*6*). Since mutation of the proton donor D96 alters the λ_{max} of M_2 but not of M_1, it is inferred that M_1 and M_2 differ in their connectivity to the two sides of the proton transport pathway (*21*). Other analyses of time-resolved visible spectra of bR have implicated up to four M intermediates in the kinetics. Drachev et al. (*22*) located two in each of two parallel pathways, with M_1 relaxing to M_2, and M'_1 to M'_2, in their respective pathways. On the other hand, Friedman et al. (*23*) concluded that the early M intermediate consists of four equilibrated substates which relax to a later M state through only one of the early substates.

FTIR spectroscopy has also been used to study M state dynamics. In films of WT-bR, in saline of undetermined concentration and pH, only a single M state was observed at all temperatures from 230 to 270 K (*24*). However, in glucose-embedded and hydrated thin films of WT-bR, FTIR spectroscopy showed accumulation of different M states at 240 and 260 K (*25, 26*). The M state that appears at the higher temperature is similar to M_N, a distinctive photocycle intermediate of the D96N mutant, with the amide band signature of the N state and a deprotonated SB (*27*). An N-like amide signature also appears in the M state of WT-bR in Gdn-HCl at room temperature (*28*).

Time-resolved spectroscopy has also been used to monitor the photoinduced back-reaction of the M species. UV−Vis spectra show two different SB reprotonation rate constants depending on the delay between the M preparation laser pulse and the M depletion laser pulse (*29, 30*). Since mutation of the proton donor D96 had no effect on these rates, apparently neither of the M components detected in this experiment is connected to the cytoplasmic side of the proton transport pathway (*29*). The sign of the photovoltage in the back-reaction also indicates reprotonation of both components from the extracellular side of the membrane (*30*). The two components are distinguished by the absence of the second, slower reacting component at low pH, suggesting that its occurrence depends on proton release from the membrane after formation of the first, faster reacting component (*30*). Meanwhile, the FTIR difference spectra of the two M components detected in the double-flash experiments show no evidence of chromophore isomerization, and only a "minute" change in the peptide backbone (*31*). This small perturbation contrasts with the large change that occurs later, in the M-to-N transition.

Since bR forms a 2D crystal in the native purple membrane patches, diffraction methods can be used to elucidate its structure. Many different conditions have been used to prepare M intermediates for diffraction experiments. In WT-bR, two structurally distinct M states have been accumulated by irradiating at two different temperatures (*26, 28, 32*). For the D96N mutant, the degree of hydration has been varied to give two structurally different M's at room temperature (*28*). N-like M states have been selected for WT-bR in Gdn-HCl or arginine at high pH (*28, 33*−*35*), and in mutants at mild pHs and temperatures (*28, 36*−*38*). The observed structures for all these M's fall roughly into two groups (*28, 39*). The most prominent difference is a tilt of the cytoplasmic end of the F-helix away from the membrane normal in the N-like group. This widens the proton uptake channel and presumably facilitates access to water. The movement of the F-helix has been seen by neutron (*33*), X-ray (*28, 34*−*36, 38*), and electron diffraction (*32, 37, 39*).

The variety of conditions that have been used to study M states makes the interpretation and comparison of results difficult. Dynamic relationships can be obtained from time-resolved spectroscopy, but the UV−Vis absorbances of the M states are very similar and lack structural information. FTIR provides a better probe of structure, but the time-resolved experiments on WT-bR have detected only minor differences in the M states. Markedly different M states have been prepared by using mutants, guanidine, dehydration, high glucose concentration, and/or low temperatures. But in the absence of relaxation studies, it is impossible to know if or how these M states are dynamically related.

Our goal is direct detection of the multiple M states, with thermal relaxation to demonstrate their sequence in the photocycle, and detailed structural information to address the mechanism of proton pumping. Using solid-state nuclear magnetic resonance (SSNMR) techniques, we have discovered up to three M's in native bR samples, M_{o1}, M_{o2}, and M_n, where the provisional subscripts 'o' and 'n' simply represent 'old' and 'new', respectively. M_n is stable at around −10 °C and coexists with the N intermediate. M_{o1} and M_{o2} are two substates of the M_o state that is routinely trapped in our lab at lower temperatures (e.g., −60 °C). We show that M_n and N follow the M_o's in the photocycle. Furthermore, we provide evidence that this transition is associated with an increase in the pK_a of the SB and a substantial change in the conformation of the peptide backbone.

MATERIALS AND METHODS

bR Samples and Preparation. The ^{15}N chemical shift of the SB is sensitive to the chromophore state and especially to protonation (*40*). Therefore, [ζ-^{15}N]Lys-bR is a good system for studying the bR photocycle and detecting new photocycle intermediates (*41*−*44*). In addition, through γ effects, the ^{13}C chemical shifts at C_{12} and C_{14} of the retinal and C_ϵ of Lys216 are good probes of the conformations of the 13 and 15 double bonds of the chromophore and therefore provide distinctive markers for various bR intermediates (*45, 46*). For detection of structural changes in the peptide backbone, carbonyl carbons are convenient reporters.

[14-^{13}C]Retinal and [12-^{13}C]retinal were incorporated into bR via bleaching and regeneration (*47, 48*). This was

accomplished by dissolving the bR in 0.5 M hydroxylamine and stirring at 37 °C while illuminating at 540 nm. After 3−4 h, the sample was completely devoid of color. The sample was then washed 3 times with 10 mM HEPES buffer (pH 7.0). A 1.1 molar excess of [14-^{13}C]retinal or [12-^{13}C]-retinal (in ethanol) was slowly added in the dark, with vigorous shaking, and the sample was stored at 0 °C in the dark overnight. The regenerated samples were then washed 10 times in 2% BSA to remove unbound retinal.

[ζ-^{15}N]Lys-bR, [ε-^{13}C,ζ-^{15}N]Lys-bR, and [1-^{13}C]Val,[^{15}N]-Pro-bR were prepared by growing *H. salinarium* (JW-3) in a defined medium similar to that of Gochauer and Kushner (*49*), except that the D-amino acids and $^{15}NH_4Cl$ were omitted. Natural-abundance amino acids were replaced in the medium with the isotopically enriched amino acids at 0.085 g/L for Lys, 0.05 g/L for Pro, and 0.33 g/L for Val. The specificity and efficiency of the incorporation of labels were followed by using radiotracers. Extraction of samples with ammonia−acetone (1:5 in volume) showed that ∼38% of the radioactivity incorporated from lysine and ∼14% of the radioactivity incorporated from valine went into lipids or retinal. However, amino acid analysis showed no scrambling of radioactivity to other amino acids in either case. The specific radioactivity indicated that ∼55% of the lysine residues and ∼72% of the valine residues incorporated the labeled amino acid provided in the medium.

bR was isolated according to standard procedure (*50*) and washed with 0.3 M Gdn-HCl at pH 10.0 at least twice before spectroscopy. Each wash was 2−3 h long, and the final wash lasted overnight. The pellet obtained by centrifuging for 1 h at 30000*g* was packed into a transparent 7 mm Sapphire crystal rotor (Doty Scientific, SC). Excess water was withdrawn from the center of the rotor after an initial spinning period in the MAS NMR probe.

In Situ Illumination. For convenient and precise trapping, samples were illuminated at low temperature directly in the probe and magnet (*41*). For the preparation of different intermediates, the only conditions that are varied are the temperature and the illumination time, intensity, and wavelengths.

Light-Adaptation. LA-bR was accumulated at 0 °C by illuminating for several hours with the entire spectrum of a 1000 W xenon lamp, filtered through 4 in. of water.

Accumulation of M_n and/or N. LA-bR was illuminated with λ > 540 nm light at −10 °C for 1 h. In 0.3 M Gdn-HCl at pH 10.0, M_n+N are present, with the former being the main product.

Accumulation of M_o. LA-bR was illuminated with λ > 540 nm at −60 °C for 1−2 h.

Thermal Relaxation. M_o relaxes to M_n and/or N at −29 °C and to LA-bR at 0 °C. M_n and/or N relaxes to LA-bR at 0 °C. All the relaxation periods were about 1 h long.

^{15}N and ^{13}C SSNMR. Basic CP/MAS experiments were performed on a custom-built spectrometer operating at 317 MHz for ^{1}H, 79.9 MHz for ^{13}C, and 32.2 MHz for ^{15}N. Spectra were acquired in the dark at −70 to −90 °C. The low temperature improves the signal-to-noise ratio and ensures that the photocycle intermediates accumulated at higher temperatures remain stable for the tens of hours required to obtain satisfactory data. Typical conditions were as follows: proton 90° pulse, 3.7 μs; recycling delay, 3 s; FID digitization size, 1024; dwell time, 20 ms; CP mixing time, 2 ms; and spinning speed, 3−4 kHz. All the ^{15}N chemical shifts were referred to $^{15}NH_4Cl$ in saturated (5.6 M) solution and the ^{13}C chemical shifts to TMS (tetramethylsilane). For ^{13}C studies of the chromophore in bR, we use difference spectroscopy (i.e., subtraction of the natural-abundance spectrum of an unlabeled sample from the spectrum of the isotopically labeled sample) (*51*). In the difference spectrum, only the signals from the labeled sites appear.

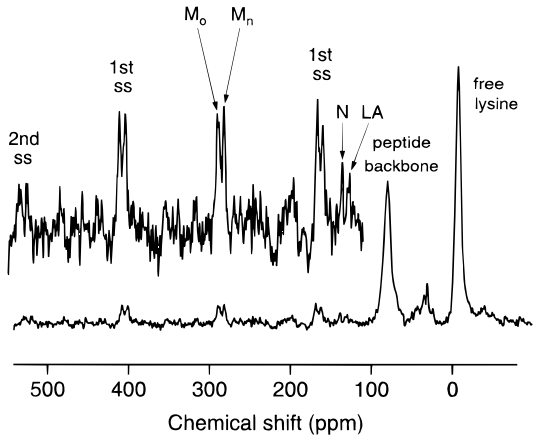

FIGURE 2: Coexistence of two M intermediates in the WT-bR photocycle, indicated by the doublet in the deprotonated SB region of the ^{15}N NMR spectrum of [ζ-^{15}N]Lys-bR. The centerbands and the first- and second-order spinning sidebands (ss) of M_n and M_o are identified in the inset. The spinning speed was 3.72 kHz.

RESULTS

[ζ-^{15}N]Lys-bR. The first NMR observation of two M intermediates comes from a two-step illumination of light-adapted [ζ-^{15}N]Lys-bR in 0.3 M Gdn-HCl at pH 10.0 with wavelengths >540 nm: for a brief period at −10 °C and then for a longer period at −60 °C. In the ^{15}N chemical shift region of deprotonated SB, a well-resolved doublet appears, together with its first- and second-order rotational sidebands (Figure 2). The downfield chemical shifts of the doublet, at 296.4 and 288.6 ppm, are characteristic of a deprotonated Schiff base nitrogen. The M state at 296.4 ppm is the one previously trapped in our lab for NMR studies, and the one at 288.8 ppm has not been observed before. We provisionally designate the old M as M_o and the new M as M_n. A small amount of the LA and N states is also discernible in the spectrum with signals at 143.4 ppm (*42*) and 150.7 ppm (*43*), respectively.

Figure 3 demonstrates the relationships between LA, M_o, and M_n. We start with DA-bR which has a doublet at 143 and 150 ppm, corresponding to bR_{568} and bR_{555}, respectively (Figure 3a). This is converted to pure bR_{568} (a singlet at 143 ppm) upon illumination at 0 °C (Figure 3b). Subsequent illumination at −10 °C with λ > 540 nm creates M_n and N intermediates coexisting with LA (Figure 3c). Thermal relaxation of the mixture at 0 °C in the dark for an hour restores the system to the resting state, bR_{568} (Figure 3d). These results indicate that M_n and N are in the photocycle of bR_{568} and that they have a thermal stability comparable to each other, which is somewhat less than bR_{568}, but much greater than M_o (which does not survive at −10 °C).

Analogous results for M_o preparation and relaxation are shown in Figure 3e,f. The only difference between Figure

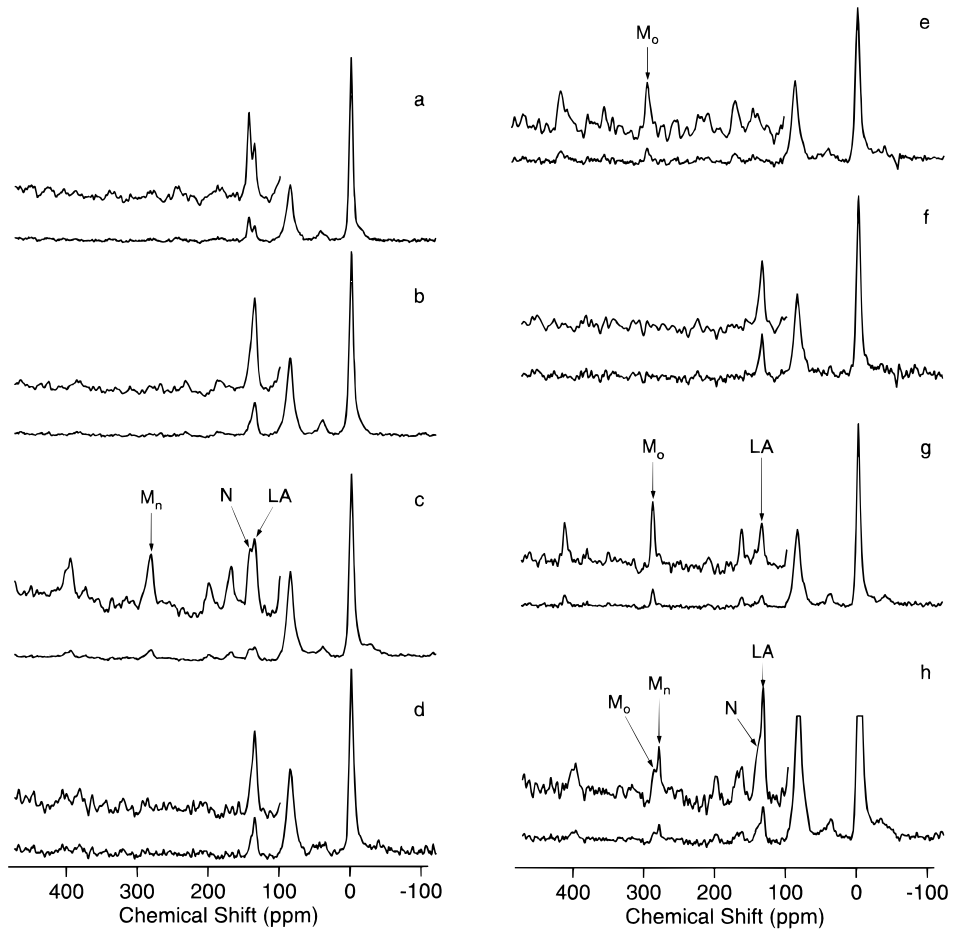

FIGURE 3: ^{15}N spectra of [ζ-^{15}N]Lys-bR showing the sequential generation and relaxation of the different states of bR in 0.3 M Gdn-HCl at pH 10.0. (a) Spectrum of DA-bR before illumination. From right (upfield) to left (downfield), the four signals are due to free lysines, the peptide backbone, and the Schiff bases in bR_{568} and bR_{555}. (b) Spectrum after light-adaptation. The bR_{555} signal is gone. (c) Result of subsequent $\lambda > 540$ nm illumination at −10 °C. A mixture of M_n, N, and LA is obtained. (d) Spectrum following relaxation of the mixture in (c) at 0 °C for 1 h in the dark. The signals of M_n and N are gone, and only bR_{568} remains [compare with (b)]. (e) Old M intermediate (M_o) is formed at −60 °C after $\lambda > 540$ nm illumination of the LA in (d). (f) Relaxation of the M_o at 0 °C reproduces LA [compare with (b) and (d)]. (g) M_o is prepared again by illumination of (f) at −60 °C, with residual LA remaining due to abbreviated illumination. (h) M_o from (g) relaxes to M_n, N, and LA after 1 h in the dark at −29 °C.

3e and Figure 3c is that the illumination temperature was set at −60 °C rather than −10 °C. The NMR spectrum of LA is obtained before $\lambda > 540$ nm illumination (Figure 3d), of M_o after $\lambda > 540$ nm illumination (Figure 3e), and of LA after thermal relaxation in the dark for 1 h at 0 °C (Figure 3f). Interestingly, when M_o is prepared again (Figure 3g) but then relaxed in the dark for 1 h at −29 °C (Figure 3h), the thermal relaxation products include M_n, N, and LA, with residual M_o owing to perhaps an insufficiently long relaxation time or an insufficiently high temperature. Further relaxation of the mixture at 0 °C for 1 h leads back to bR_{568}. The results indicate that M_n and N derive from M_o and are more stable than M_o. The isolation of M_o at −60 °C indicates an interception of M_o prior to M_n and N in the photocycle of bR_{568}.

[14-^{13}C]ret,[ϵ-^{13}C,ζ-^{15}N]Lys-bR. Further studies of the two M states have been carried out using [14-^{13}C]ret, [ϵ-^{13}C,ζ-^{15}N]Lys-bR in order to get ^{13}C chemical shift information. Due to a γ effect, the [14-^{13}C]ret and [ϵ-^{13}C]-Lys216 chemical shifts are sensitive to the configuration of the C=N bond. Through conjugation, the chemical shift of [14-^{13}C]ret is also sensitive to interactions that affect the electronic states of the polyene system.

Figure 4 shows the ^{13}C difference spectra for the states seen in Figure 3. Again, DA (Figure 4a) is converted to LA (Figure 4b). After illumination of LA with $\lambda > 540$ nm at −10 °C (Figure 4c), a mixture of LA, M_n, and N is again observed. The LA signals are at 53 and 122.3 ppm for [ϵ-^{13}C]Lys216 and [14-^{13}C]ret, respectively (*46*). The N signals are at 53 and 115 ppm for [ϵ-^{13}C]Lys216 and [14-^{13}C]ret, respectively (*43*). Therefore, the signals at 60.4 and 124.6 ppm for [ϵ-^{13}C]Lys216 and [14-^{13}C]ret, respectively, are from M_n. Since the intensities (summed over all sidebands) in the previous ^{15}N spectra showed M_n to be the main component of the mixture obtained under these conditions (Figure 3c), it is not surprising that the ^{13}C signals of the N intermediate are weaker than those of M_n (Figure 4c). Warming M_n+N to 0 °C again restores the LA state (Figure 4d), and reilluminating at −60 °C produces M_o (Figure 4e).

The ^{13}C chemical shifts for M_o are as observed previously (*43, 46*). However, with improved S/N and resolution, two isomers can be detected in the M_o intermediate from a splitting in the [14-^{13}C]ret peak. The doublet also appears in the sidebands, and is reproducible in repeated experiments. In retrospect, the presence of two isomers explains why the

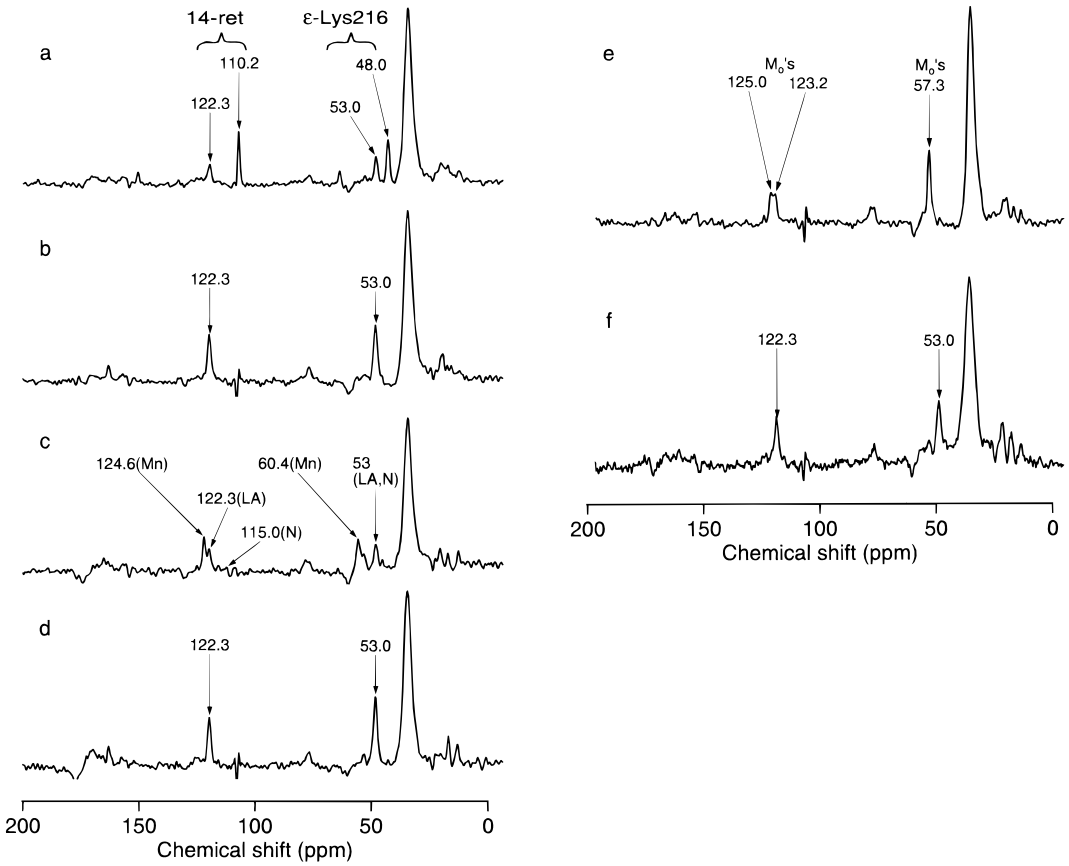

FIGURE 4: ^{13}C difference (labeled minus natural abundance) spectra for [14-^{13}C]ret,[ϵ-^{13}C]Lys-bR in 0.3 M Gdn-HCl at pH 10.0. (a) bR_{568} and bR_{555} in DA-bR. (b) Pure bR_{568} in LA. (c) Mixture of M_n+N+LA obtained by illumination of LA with λ > 540 nm at −10 °C. The assignments of the lines are as marked (see text). (d) LA recovered by the relaxation of M_n+N at 0 °C. (e) Pure M_o generated by illumination of LA with λ > 540 nm at −60 °C. The [14-^{13}C]ret signal at about 124 ppm is split although the [ϵ-^{13}C]Lys signal at 57.3 ppm remains a sharp singlet. (f) LA recovered by relaxation of M_o at 0 °C.

[14-^{13}C]ret peak for M_o has always been broad. In fact, a close examination of the spectrum of M_o obtained by Farrar et al. (*46*) suggests doublets rather than broad singlets in the centerband and sidebands. We designate the two states, at 123.2 and 125.0 ppm, M_{o1} and M_{o2}, respectively.

[12-^{13}C]ret-bR. Another method for potentially distinguishing the two M states is to probe the configuration around the C_{13}═C_{14} double bond of retinal chromophore using [12-^{13}C]ret-bR. The ^{13}C chemical shift of this retinal label is sensitive to the cis/trans isomerization around the C_{13}═C_{14} bond due to the γ-effect (*45*, *52*).

Figure 5 shows the difference spectra of [12-^{13}C]ret-bR. On the top is the spectrum of light-adapted bR with the [12-^{13}C]ret resonance at 134.3 ppm (Figure 5a). After illumination of LA with λ > 540 nm at −10 °C (Figure 5b), a mixture of LA, M_n, and N is again observed. At 10 ppm upfield from the weak residual LA signal at 134.3 ppm, the M_n and N resonances are very close, resulting in a broad signal at 124.5 ppm. After relaxation at 0 °C, reillumination with λ > 540 nm at −60 °C produces M_o (Figure 5c). The M_o chemical shift at 125.7 ppm is downfield by 1.2 ppm from the M_n+N resonance. This peak is much broader than that of LA, which could be further evidence of two M_o subspecies.

[1-^{13}C]Val,[^{15}N]Pro-bR. LA, M_o, and M_n+N are also found to differ from each other in the structure of the protein backbone. Figures 6 and 7 show ^{13}C CPMAS spectra of [1-^{13}C]Val,[^{15}N]Pro-bR in the LA, M_o, and M_n+N states.

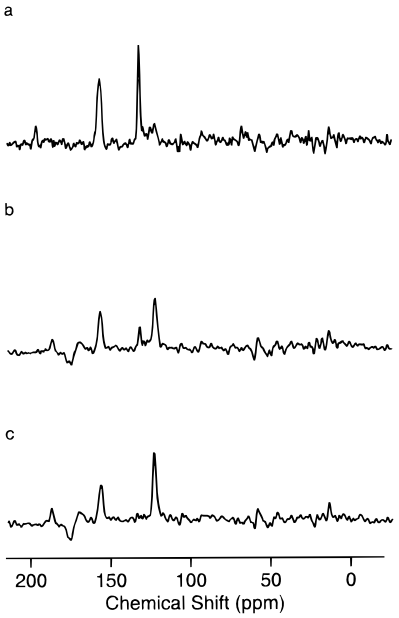

FIGURE 5: ^{13}C difference (labeled minus natural abundance) spectra of [12-^{13}C]ret-bR in 0.3 M Gdn-HCl at pH 10.0. (a) Pure bR_{568} in LA. (b) Mixture of M_n+N+LA obtained by illumination of LA with λ > 540 nm at −10 °C. (c) Pure M_o generated by illumination of LA with λ > 540 nm at −60 °C.

Of the 21 valines, there is a net change of only a small number. This is best seen in the LA − M_o and LA − (M_n+N) difference spectra at the bottom of Figures 6 and

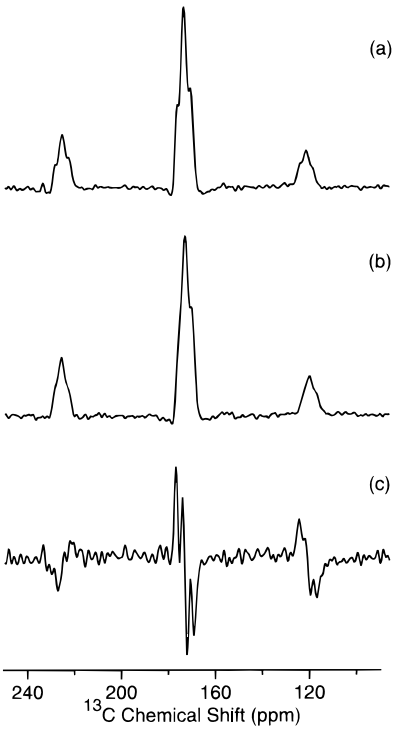

FIGURE 6: ^{13}C spectra of [1-^{13}C]Val,[^{15}N]Pro-bR, in 0.3 M Gdn-HCl at pH 10.0. (a) LA. (b) M_o. (c) The difference LA − M_o.

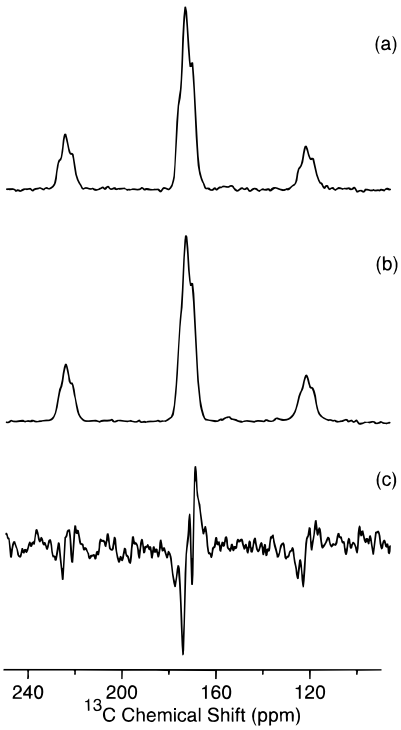

FIGURE 7: As Figure 6 but for M_n+N. (a) LA. (b) M_n+N+LA. (c) The difference LA − (M_n+N+LA).

7. In M_o, at least two valines have moved downfield relative to LA, while in M_n+N these valines have relaxed and at least two other valines have moved upfield relative to LA. This indicates that the greatest difference is between M_o and (M_n+N).

DISCUSSION

The present study is restricted to intact purple membranes of wild-type bR in 0.3 M Gdn-HCl at pH 10.0. No mutants are involved, nor have the membranes been dehydrated or solubilized by detergents. Although guanidine is a denaturant for most proteins, the native structure of bR is not perturbed at these guanidine concentrations according to any reported spectroscopic measures. Furthermore, bR has been found to pump protons in 8 M Gdn-HCl in the pH range from 4.7 to 9.8 (*53*). Therefore, the photocycle observed in the present work is energy transducing. The advantage of guanidine for studying the mechanism of proton transport is that reprotonation of the SB is slowed, presumably by interfering with the proton uptake in the cytoplasmic channel. This extends the lifetime of the M state. The high pH also reduces the reprotonation rate and increases the barrier for the M→N transition.

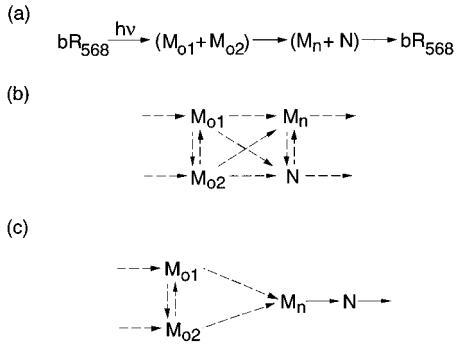

FIGURE 8: Reaction pathways for the photocycle of native wild-type bR in 0.3 M Gdn-HCl at pH 10.0. (a) The established overall scheme. The left and right arrows are known to represent multiple steps, and the center arrow may also. (b) Possibilities in the central segment of the photocycle assuming that M_n+N represents an equilibrium mixture. One or both of the left reactions must occur, one or more of the middle reactions must occur, and one or both of the right reactions must occur. (c) Possibilities in the center segment of the photocycle assuming that M_n+N represents a steady-state mixture with N following M_n. One or both of the leftmost reactions must occur, and one or both of the left of center reactions must occur.

The occurrence of the various bR states observed here depends only on variations in the illumination and the temperature. To study the proton motive photocycle under conditions with a long M lifetime, we use only light of $\lambda >$ 540 nm. This is outside the absorption band for M and avoids the generation of photoproducts of M. The results of illumination of bR_{568} (LA) with $\lambda >$ 540 nm depend on the temperature. At −60 °C, we find that M_{o1} and M_{o2} accumulate. The barrier for thermal relaxation of M_{o1} and M_{o2} at this temperature must therefore be greater than for all preceding steps of the photocycle. At −10 °C, where M_{o1} and M_{o2} are less stable, M_n and N accumulate instead. The barrier for thermal relaxation of M_n and N must therefore be higher at this temperature than that of M_{o1} and M_{o2}.

The proof that all these intermediates are on the same pathway comes from studies of thermal relaxation in the dark. While all the observed photocycle intermediates relax back to bR_{568} in an hour at 0 °C, the mixture of M_{o1} and M_{o2} relaxes to a mixture of M_n and N in an hour at −29 °C. M_{o1} and M_{o2} must therefore precede M_n and N in the temporal sequence, and the different proportions in the two mixtures preclude the possibility of two separate pathways between the components. We therefore deduce the overall reaction sequence shown in Figure 8a.

What is not yet clear is the role of M_{o1} vs M_{o2} in the first mixture and M_n vs N in the second mixture. In principle,

Table 1: Chemical Shifts for Observed Forms of bR

	12-^{13}C	14-^{13}C	ϵ-^{13}C	SB-^{15}N
bR_{555}	124.2	110.2	48.0	150.7
bR_{568}	134.3	122.3	53.0	143.4
M_o	125.7	125.0, 123.2	57.3	296.4
M_n	124.5	124.6	60.4	288.8
N[a]	124.4	115.0	53.0	150.7

[a] Data from Lakshmi et al. (1994).

each mixture may represent an equilibrium between the two components or a steady-state population for a sequence in which one component precedes the other. However, for $M_{o1}+M_{o2}$ to represent a steady-state population requires recycling one to the other through M_n+N. But, since M_n+N accumulate at −10 °C, we know they would not recycle efficiently at −60 °C. Thus, the $M_{o1}+M_{o2}$ mixture must represent an equilibrium between these two species. This is consistent with the findings so far that the difference between M_{o1} and M_{o2} is subtle and localized mainly to the C_{14} of the retinal. The analogous argument cannot be made for the M_n+N mixture, and we must allow for the possibility that this represents a steady-state population or an equilibrium population. In the former case, it is expected that M_n precedes N in the sequence. These possibilities are illustrated in Figure 8b,c.

Some insights into the similarities and differences between M_o and M_n can be drawn from the chemical shifts summarized in Table 1. In both M_o and M_n, [ϵ-^{13}C]Lys and [14-^{13}C]ret are deshielded relative to LA and N, due to the deprotonation of the SB that is most clearly reflected in the ^{15}N chemical shifts. The similarity between [ϵ-^{13}C]Lys and [14-^{13}C]ret chemical shifts of M_o and M_n indicates that M_n, like M_o, has a C=N anti conformation. Internuclear distance measurements have unambiguously established that the C=N conformation is syn for bR_{555} and anti for bR_{568} (*54*) and M_o (*55*). M_n must also be C=N anti because steric interactions in the C=N syn structure would cause a 5−7 ppm upfield shift from the M_o chemical shifts. According to resonance Raman results, the C=N anti conformation is also shared by the K, L, and N intermediates of the photocycle (*16, 56*−*58*). However, NMR results suggest that this bond is strained in L and relaxed in N (*41*). The chemical shifts of [12-^{13}C]ret in M_o and M_n are also similar to each other. About 10 ppm upfield of bR_{568}, like those of bR_{555} and N, they reflect a 13-*cis*-retinal conformation. This is consistent with resonance Raman results indicating that all the photointermediates from J_{625} to N_{520} share the 13-*cis*-retinal conformation (*16, 56*−*58*).

Although the SB nitrogen is strongly deshielded in both M_o and M_n, due to the paramagnetic effect of the lone pair electrons, there is a substantial difference in the ^{15}N chemical shifts between them, such that the SB nitrogen becomes more shielded when M_o relaxes to M_n (see Table 1). The direction of these changes is consistent with preparation for reprotonation of the SB (*18, 59*). Studies of various para-substituted benzalanilines show that increased shielding of the nitrogen in unprotonated Schiff bases, over a range of 30 ppm (*60, 61*), correlates with increased base strength (*62*). A further increase in shielding occurs with hydrogen bonding (*60*). For example, a 9 ppm upfield shift is observed on transfer of a relatively basic benzalaniline from chloroform solution to methanol solution. Both stronger basicity and stronger hydrogen bonding would improve the prospects for reprotonation of M_n over that of M_o.

Another important difference between M_o and M_n shows up in the peptide backbone as sampled by the carbonyl carbons of the valine residues. These probes indicate that the structure changes more between the two M mixtures than between LA and either M mixture. In particular, energy is seen to be moving through the protein, with relaxation of residues in M_n that were perturbed in M_o and perturbation of residues in M_n that were unperturbed in M_o. Such a major structural change is consistent with the relatively large activation barrier between M_o and M_n, and the greater stability of M_n compared to M_o.

With increased pK_a and/or H-bonding of the SB, and a substantial change in protein structure, the demonstrated $M_o \rightarrow M_n$ transition has the elements required for a reprotonation switch. The change in protein structure, combined with the relaxation of the chromophore that occurs between L and N states (*41*), has the potential to switch the connectivity of the Schiff base from one side of the membrane to the other, while the increase in pK_a and/or H-bonding will encourage reprotonation. Thus, M_o and M_n are good candidates for early and late M (or what has been called M_1 and M_2 or M1 and M2).

Based on the similarity of the M_n and N states in thermal stability, M_n may resemble the N-like M states trapped by several groups. In particular, the M_{260K} state trapped by Vonck et al. (*26*) in glucose-embedded WT-bR is also relatively stable and has a protein structure similar to N, but different from the M they obtained at 240 K (*39*). The M_n state that we observe may also be related to the M_N state observed in the D96N mutant, where proton uptake is significantly retarded (*27*). In our experiments, the combination of 0.3 M Gdn-HCl and pH 10.0 may inhibit SB reprotonation sufficiently in WT-bR to allow observation of M_N. Neutron diffraction (*33*), X-ray diffraction (*28, 34, 35*), electron diffraction (*32*), and FTIR spectroscopy (*24*−*28, 63*) have all demonstrated N-like M states in WT-bR. The present NMR study goes beyond the earlier studies in not only confirming the similar thermal stability of M_n and N but also demonstrating that M_n is a relaxation product of M_o in WT-bR, and providing evidence that the SB has a higher pK_a and/or stronger H-bonding in M_n than in M_o.

M_o is much less stable than M_n under the experimental conditions used in this study. As such, M_o may resemble the M_{240K} trapped in glucose-embedded WT-bR (*26*) because M_{240K} can also be prepared in pure form and is stabilized at lower temperatures than M_{260K}. However, different markers for M_o and M_{240K} (or, for that matter, M_n and M_{260K}) make it difficult to compare them. The assignments of M_1 in other diffraction studies are based largely on structural contrast with an N-like M_2 species. This is reasonable in terms of a protein structural change between the non-N-like M_1 and the N-like M_2 states. Relative to the resting LA state of bR, the M_1 state shows structure changes in the G-helix (*28, 32, 37*), presumably because of its direct bonding to the isomerized retinal chromophore through the SB linkage. In the M_2 and the N states, the F-helix is tilted away from the membrane normal, producing an opening in the cytoplasmic end of the proton channel (*28, 37*−*39, 64*). However, the relationship between the non-N-like and N-like M states has not been demonstrated by relaxation from one to the other

in the dark. Nor is the functionally significant change in the chemical properties of the SB accessible in the diffraction studies. The present NMR work links the thermal relaxation of M to changes in both the protein backbone and the SB chemistry.

Our observation of the two subtly different substates of M_o may be related to the two subtly different M's detected in studies of the photo-induced back-reaction (*29*−*31*), and thus to proton release from the membrane (*30*). This possibility could be tested by further NMR studies monitoring the pH dependence of the ratios of the two M_o substates down to the pHs at which the slow component in the M back-photoreaction disappears, putatively because proton release is delayed until later in the photocycle. However, the NMR results already in hand suggest that the two M_o substates are in equilibrium with each other and therefore do not represent an irreversible step in the photocycle. Thus, if they are associated with proton release from the membrane, that release does not contribute to the vectoriality of proton transport, even at high pH. It is the relaxation from M_o to M_n that has the potential for irreversibility and vectoriality.

CONCLUSIONS

Three M intermediates have been observed in the proton motive photocycle of native wild-type bR using solid-state ^{15}N and ^{13}C NMR. With high resolution and S/N, the previously observed M_o, produced by $\lambda > 540$ nm illumination of bR_{568} in 0.3 M Gdn-HCl at −60 °C, is found to have at least two subtly distinct substates. Warming M_o to −29 °C in the dark yields a new M intermediate, M_n, along with N. M_n and N, in turn, relax to bR_{568} at 0 °C in the dark. This defines a photocycle pathway: LA→M_o→(M_n+N)→LA. Like M_o and N, M_n has a C═N anti SB configuration and a 13-*cis*-retinal conformation. The M_o→(M_n+N) transition is a strong candidate for the long-sought "reprotonation switch" because increased shielding of the SB nitrogen indicates conditions favorable for reprotonation, and changes in the carbonyl chemical shifts of several valine residues indicate a larger protein conformational change between M_o and M_n than between LA and either M state, including the replacement of early perturbations by others at different locations.

ACKNOWLEDGMENT

We thank Barry Snider for helpful discussions.

REFERENCES

1. Gerwert, K., Hess, B., & Engelhard, M. (1990) *FEBS* Lett. *261*, 449−454.
2. Ames, J. B., & Mathies, R. A. (1990) *Biochemistry 29*, 7181−7190.
3. Druckman, S., Heyn, M. P., Lanyi, J. K., Ottolenghi, M., & Zimanyi, L. (1993) *Biophys. J. 65*, 1231−1234.
4. Milder, S. J. (1991) *Biophys. J. 60*, 440−446.
5. Varo, G., & Lanyi, J. K. (1990) *Biochemistry 29*, 2241−2250.
6. Varo, G., & Lanyi, J. K. (1991) *Biochemistry 30*, 7165−7171.
7. Varo, G., & Lanyi, J. K. (1991) *Biochemistry 30*, 5008−5015.
8. Varo, G., & Lanyi, J. K. (1991) *Biochemistry 30*, 5016−5022.
9. Varo, G., & Lanyi, J. K. (1991) *Biophys. J. 59*, 313−322.
10. Brown, L. S., Sasaki, J., Kandori, H., Maeda, A., Needleman, R., & Lanyi, J. K. (1995) *J. Biol. Chem. 270*, 27122−27126.
11. Braiman, M. S., Bousche, O., & Rothschild, K. J. (1991) *Proc. Natl. Acad. Sci. U.S.A. 88*, 2388−2392.
12. Gerwert, K., Souvignier, G., & Hess, B. (1990) *Proc. Natl. Acad. Sci. U.S.A. 87*, 9774−9778.
13. Otto, H., Marti, T., Holz, M., Mogi, T., Stern, L. J., Engel, F., Khorana, H. G., & Heyn, M. P. (1990) *Proc. Natl. Acad. Sci. U.S.A. 87*, 1018−1022.
14. Rothschild, K. J. (1992) *J. Bioenerg. Biomembr. 24*, 147−167.
15. Oesterhelt, D., Tittor, J., & Bamberg, E. (1992) *J. Bioenerg. Biomembr. 24*, 181−192.
16. Fodor, S. P. A., Ames, J. B., Gebhard, R., Van den Berg, E. M. M., Stoeckenius, W., Lugtenburg, J., & Mathies, R. A. (1988) *Biochemistry 27*, 7097−7101.
17. Henderson, R., Baldwin, J. M., Ceska, T. A., Zemlin, F., Beckmann, E., & Downing, K. H. (1990) *J. Mol. Biol. 213*, 899−929.
18. Lanyi, J. K. (1992) *J. Bioenerg. Biomembr. 24*, 169−179.
19. Varo, G., Zimanyi, L., Chang, M., Ni, B., Needleman, R., & Lanyi, J. (1992) *Biophys. J. 61*, 820−826.
20. Zimanyi, L., Varo, G., Chang, M., Ni, B., Needleman, R., & Lanyi, J. (1992) *Biochemistry 31*, 8535−8543.
21. Zimanyi, L., Cao, Y., Chang, M., Ni, B., Needleman, R., & Lanyi, J. (1992) *Photochem. Photobiol. 56*, 1049−1055.
22. Drachev, L. A., Kaulen, A. D., & Komrakov, A. Y. (1994) *Biochemistry (Moscow) 59*, 95−102.
23. Friedman, N., Gat, Y., Sheves, M., & Ottolenghi, M. (1994) *Biochemistry 33*, 14758−14767.
24. Ormos, P., Chu, K., & Mourant, J. (1992) *Biochemistry 31*, 6933−6937.
25. Perkins, G. A., Liu, E., Burkard, F., Berry, E. A., & Glaeser, R. M. (1992) *J. Struct. Biol. 109*, 142−151.
26. Vonck, J., Han, B.-G., Burkard, F., Perkins, G. A., & Glaeser, R. M. (1994) *Biophys. J. 67*, 1173−1178.
27. Sasaki, J., Shichida, Y., Lanyi, J. K., & Maeda, A. (1992) *J. Biol. Chem. 267*, 20782−20786.
28. Sass, H. J., Schachowa, I. W., Rapp, G., Koch, M. H. J., Oesterhelt, D., Dencher, N. A., & Bueldt, G. (1997) *EMBO J. 16*, 1484−1491.
29. Druckmann, S., Friedman, N., Lanyi, J. K., Needleman, R., Ottolenghi, M., & Sheves, M. (1992) *Photochem. Photobiol. 56*, 1041−1047.
30. Dickopf, S., & Heyn, M. P. (1997) *Biophys. J. 73*, 3171−3181.
31. Hessling, B., Herbst, J., Rammelsberg, R., & Gerwert, K. (1997) *Biophys. J. 73*, 2071−2080.
32. Han, B.-G., Vonck, J., & Glaeser, R. M. (1994) *Biophys. J. 67*, 1179−1186.
33. Dencher, N. A., Dresselhaus, D., Zaccai, G., & Bueldt, G. (1989) *Proc. Natl. Acad. Sci. U.S.A. 86*, 7876−7879.
34. Dencher, N. A., Heberle, J., Bark, C., Koch, M. H. J., Rapp, G., Oesterhelt, D., Bartels, K., & Bueldt, G. (1991) *Photochem. Photobiol. 54*, 881−887.
35. Nakasako, M., Kataoka, M., Amemiya, Y., & Tokunaga, F. (1991) *FEBS Lett. 292*, 73−75.
36. Koch, M. H. J., Dencher, N. A., Oesterhelt, D., Ploehn, H. J., Rapp, G., & Bueldt, G. (1991) *EMBO J. 10*, 521−526.
37. Subramaniam, S., Gerstein, M., Oesterhelt, D., & Henderson, R. (1993) *EMBO J. 12*, 1−8.
38. Kamikubo, H., Kataoka, M., Varo, G., Oka, T., Tokunaga, F., Needleman, R., & Lanyi, J. K. (1996) *Proc. Natl. Acad. Sci. U.S.A. 93*, 1386−1390.
39. Vonck, J. (1996) *Biochemistry 35*, 5870−8.
40. Harbison, G. S., Herzfeld, J., & Griffin, R. G. (1983) *Biochemistry 22*, 1−5.
41. Hu, J. G., Sun, B. Q., Petkova, A. T., Griffin, R. G., & Herzfeld, J. (1997) *Biochemistry 36*, 9316−9322.
42. De Groot, H. J. M., Harbison, G. S., Herzfeld, J., & Griffin, R. G. (1989) *Biochemistry 28*, 3346−3353.
43. Lakshmi, K. V., Farrar, M. R., Raap, J., Lugtenburg, J., Griffin, R. G., & Herzfeld, J. (1994) *Biochemistry 33*, 8853−8857.
44. Smith, S. O., Courtin, J., Van den Berg, E., Winkel, C., Lugtenburg, J., Herzfeld, J., & Griffin, R. G. (1989) *Biochemistry 28*, 237−243.
45. Smith, S. O., De Groot, H. J. M., Gebhard, R., Courtin, J. M. L., Lugtenburg, J., Herzfeld, J., & Griffin, R. G. (1989) *Biochemistry 28*, 8897−8904.

46. Farrar, M. R., Lakshmi, K. V., Smith, S. O., Brown, R. S., Raap, J., Lugtenburg, J., Griffin, R. G., & Herzfeld, J. (1993) *Biophys. J. 65*, 310−315.
47. Hamanaka, T., Hiraki, K., & Kito, Y. (1986) *Photochem. Photobiol. 44*, 75−78.
48. Oesterhelt, D., & Schuhmann, L. (1974) *FEBS Lett. 44*, 262−265.
49. Gochauer, M. B., & Kushner, D. (1969) *Can. J. Microbiol. 15*, 1157−1165.
50. Oesterhelt, D., & Stoeckenius, W. (1974) *Methods Enzymol. 31*, 667−678.
51. de Groot, H. J. M., Copie, V. C., Smith, S. O., Allen, P. J., Winkel, C., Lugtenburg, J., Herzfeld, J., & Griffin, R. G. (1988) *J. Magn. Reson. 77*, 251.
52. Harbison, G. S., Smith, S. O., Pardoen, J. A., Mulder, P. P. J., Lugtenburg, J., Herzfeld, J., Mathies, R., & Griffin, R. G. (1984) *Proc. Natl. Acad. Sci. U.S.A. 81*, 7106.
53. Yoshida, M., Ohono, K., Takeuchi, Y., & Kagawa, Y. (1977) *Biochem. Biophys. Res. Commun. 75*, 1111−1116.
54. Thompson, L. K., McDermott, A. E., Raap, J., van der Weilen, C. M., Lugtenburg, J., Herzfeld, J., & Griffin, R. G. (1992) *Biochemistry 31*, 7931.
55. Lakshmi, K. V., Auger, M., Raap, J., Lugtenburg, J., Griffin, R. G., & Herzfeld, J. (1993) *J. Am. Chem. Soc. 115*, 8515.
56. Smith, S. O., Hornung, I., van der Stern, R., Pardoen, J. A., Braiman, M., Lugtenburg, J., & Mathies, R. (1986) *Proc. Natl. Acad. Sci. U.S.A. 83*, 967−971.
57. Braiman, M. S., & Mathies, R. (1982) *Proc. Natl. Acad. Sci. U.S.A. 79*, 403−407.
58. Fodor, S. P. A., Pollard, W. T., Gebhard, R., Van den Berg, E. M. M., Lugtenburg, J., & Mathies, R. A. (1988) *Proc. Natl. Acad. Sci. U.S.A. 85*, 2156−2160.
59. Rousso, I., Friedman, N., Sheves, M., & Ottolenghi, M. (1995) *Biochemistry 34*, 12059−12065.
60. Westerman, P. W., Botto, R. E., & Roberts, J. D. (1978) *J. Org. Chem. 43*, 2590−2596.
61. Yuzuri, T., Wada, H., Suezawa, H., & Hirota, M. (1994) *J. Phys. Org. Chem. 7*, 280−286.
62. Weinstein, J., & McIninch, E. (1960) *J. Am. Chem. Soc. 82*, 6064−6067.
63. Ormos, P. (1991) *Proc. Natl. Acad. Sci. U.S.A. 88*, 473−477.
64. Radionov, A. N., & Kaulen, A. D. (1997) *FEBS Lett. 409*, 137−140.

BI973168E